XV International Conference on Computational Plasticity. Fundamentals and Applications
COMPLAS 2019
E. Oñate, D.R.J. Owen, D. Peric, M. Chiumenti & Eduardo de Souza Neto (Eds)

ANALYSIS OF SPINNER STRAIGHTENING UTILIZING THE FINITE ELEMENT METHOD

TAKASHI KUBOKI[*], KEIICHIRO KAWASAKI[†], SHOHEI KAJIKAWA[†], HIROMICHI MATSUMURA[††], TETSUSHI ONO[††] and HIKARU SEIMIYA[††]

[*] Department of Mechanical Engineering & Intelligent Systems
The University of Electro-Communications
1-5-1 Chofu Gaoka, Chofu-shi, Tokyo, 182-8585, Japan
e-mail: kuboki@mce.uec.ac.jp - web page: http://www.mt.mce.uec.ac.jp/

[†] Department of Mechanical Engineering & Intelligent Systems
The University of Electro-Communications
1-5-1 Chofu Gaoka, Chofu-shi, Tokyo, 182-8585, Japan

[††] Shimomura Tokushu Seiko Co.,Ltd.
668-1 Matsuomachi Kashikehongo, Sammu-shi, Chiba, 289-1537, Japan
web page: http://www.sts-shimomura.com/

Key words: Spinner, Straightener, Straightness, Warp, Moment, Curvature

Abstract. This paper presents analysis methods utilizing the Finite Element Method for spinner straightening, and shows a guideline for optimum conditions. Two types of analysis methods were composed. Model [F-Expl], "full actual model with explicit scheme", considers the rotational movement of dies as the actual process using the explicit scheme. Model [BndCr], "a model carrying out fundamental analysis on one cross section based on simple bending in the Finite Element Method (FEM)", uses the FEM only for calculation of simple bending without rotation for obtaining the deformed bar shape. A series of experiments were conducted in an actual production line as well as the analyses by Model [F-Expl] and [BndCr]. The examination mainly focused upon the effect of straightening intensity by changing the die positions. The experimental and analytical results show some mechanism of straightening and a basic guideline for the optimum working condition.

1 INTRODUCTION

Straightening is located at the end of manufacturing process for bars and wire rods, and determines the quality of the final product. The requirement to the dimensional precision of bars and wire rods are getting stricter due to the recent trend of requirements to the final products which use the bars and wire rods, and then the role of straightening process is getting more important. Figure 1 shows the process line of bars. The initial bar is unwound from the coils on the supply stand, and drawn before the line of straitening processes. The straightening line is composed of a couple of processes, which includes spinner, polishing and two-roll straighteners. These straightening processes would collaboratively determine the quality of the bars, and the spinner is located at the first of the three processes.

There are few research works for spinner, though there are many for the final process, like two-roll straighter. Yanagihashi et al. [1] and Mutrux et al. [2] tried to apply the FEM to solid-bar straightening with deciding the deformed shape in advance. Furugen composed a fundamental analysis for tube straightening considering axial deformation at first, followed by the consideration of cross-sectional deformation [3]. Kuboki et al. composed a FEM model applying the implicit scheme for three-stand tube straightening [4]. Wu et al. carried out theoretical approach for analyzing the mechanism of two-roll straightener [5]. However, all the above works focused upon the final process in the production line without knowing phenomena in the first process, that is spinner straightening. Although Tsurumi et al. conducted a study on a spinner-like machine, the material was a very thin wire and the study is not so general [6].

The present study focuses upon the spinner straightening, which is the first process and may plays an important role in the production line. Analysis methods are composed utilizing the Finite Element Method for proposing a guideline for optimum conditions. Two types of analysis methods are shown. Model 1, ”full actual model with explicit scheme [F-Expl]”, considers the rotational movement of dies as the actual process using the explicit scheme. Model 2, ”a model carrying out fundamental analysis on one cross section based on simple bending in FEM [BndCr]”, uses the FEM only for calculation of simple bending without rotation for obtaining the deformed bar shape. A series of experiments were conducted in an actual production line as well as the analyses by Model [F-Expl] and [BndCr]. The examination mainly focused upon the effect of straightening intensity by changing the die positions for showing mechanism in spinner straightening and a guideline for the optimum working condition.

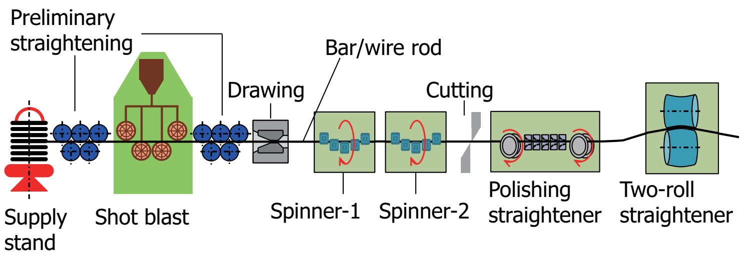

Figure 1: Process line for bars and wire rods

2 CONDITION FOR SPINNER

Figure 2 shows a schematic illustration of spinner. Only the second spinner [Spinner-2] (see Fig. 1) was used in this study. The die positions h_i ($i = 1 \cdots 5$) was defined so that the h_i should be zero when the dies contact with a completely straight bar without any load. The sign (positive/negative) of h_i was defined as shown in the figure. The die positions h_i determine the bending intensity during straightening. The detailed condition on the die positions are shown in Table 1. Condition [A] is intuitively expected to have the strongest straightening effect.

Table 2 shows the drawing condition in advance of spinner straightening. Coils of lead-free free-cutting steel was annealed, and drawn. Two-pass drawing was conducted under the condition [a], and the area reduction at the second pass was set to be around 1 % so that the residual stress should be leveled to almost zero as clarified in the literature [7]. Conventioal one-pass drawing was employed for (b) so that the residual stress might generate. The difference between conditions [a] and [b] would show the effect of residual stresses on straightening. Table 3 shows other working conditions.

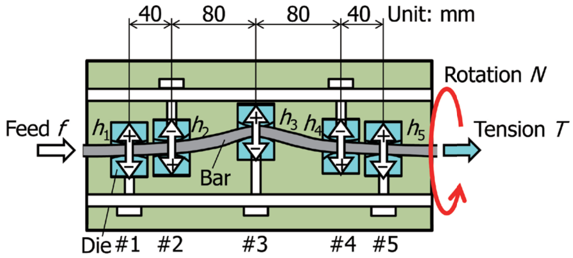

Figure 2: Composition of spinner straightener

Table 1: Die position for spinner straightening

	Position h_i/mm ($i = 1 \cdots 5$)				
[A]	0	-2.25	11.0	-2.25	0
[B]	0	-1.875	10.0	-1.875	0
[C]	0	-1.55	9.0	-1.55	0
[D]	0	-1.3	8.0	-1.3	0
[E]	0	-1.1	7.0	-1.1	0
[F]	0	-0.97	6.0	-0.97	0
[G]	0	-0.92	5.5	-0.92	0

Table 2: Drawing condition before spinner straightening

	Initial		Die inside diameter	
	Diameter d_0/mm	Heat treat	1st d_1/mm	2nd d_b/mm
[a]	7.0	Anneal	6.08	6.05
[b]	7.0	Anneal	-	6.05

Material: Lead-free free-cutting steel
Flow stress (after spinner straightening):
$\sigma = 855(\varepsilon + 0.11)^{0.089}$

Table 3: Working condition

Feed pitch f/mm $\cdot$ rev^{-1}	9.52
Initial cuvature c_0/mm $^{-1}$	8.8 $\times 10^{-5}$

3 ANALYTICAL MODELS

3.1 Full explicit scheme model [F-Expl]

Two analytical models were composed, and the detailed settings are explained in this section. Figure 3 shows the composition of spinner in the Finite Element Analysis (FEA). Guides and rollers were introduced as well as the bar and the dies. Residual stresses are assumed to be zero in the analyses in this study.

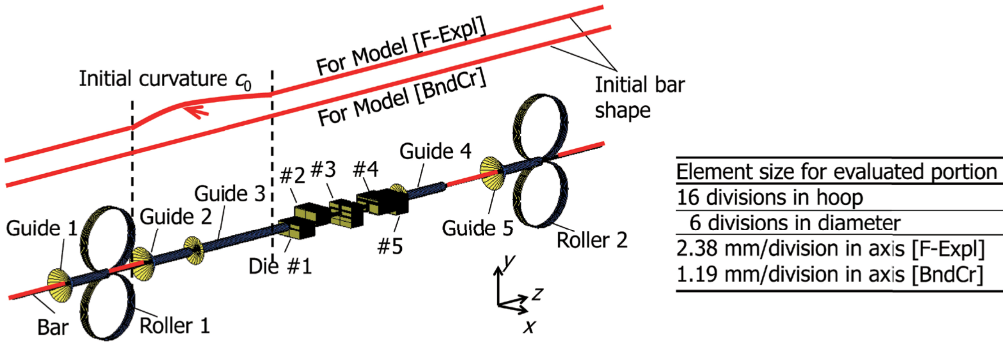

Figure 3: Model in FEA

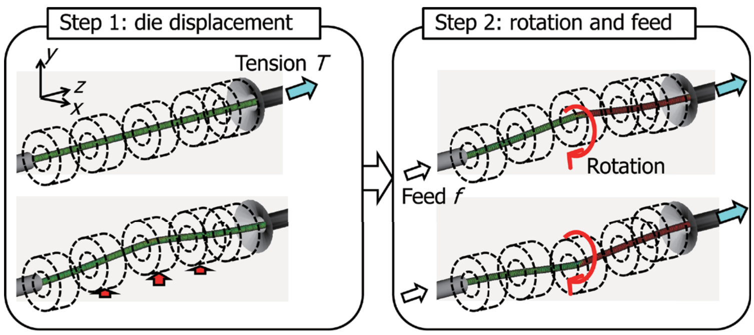

Figure 4: Analysis steps in model [F-Expl]

The first model (F-Expl, full explicit) almost fully reproduced the movement of spinner straightening using the explicit scheme. The analysis was carried out by two steps as shown in Figure 4. The bar was set through Guide 1 to roller 2 via dies #1 – #5, and the front tension T was applied. The dies gradually moved to the target position of $h_i(i = 1, \cdots, 5)$ at Step 1. At Step 2, the rotational movement was given to the dies, while feeding movement was given to the bar end. Although Model [F-Expl] would not be as precise as a model with the implicit scheme, it can consider the centrifugal force and the convergence would be stable. An initial curvature c_0 was given to the bar between the Roller 1 and Die #1, and the curvature was evaluated at the same portion of the bar during and after the spinner straightening.

The FEA was carried out using the commercial code ELFEN, which was developed by Rockfield Software Limited, Swansea. A von Mises' yield criterion was adopted, and the normality principle was applied to the flow rule. Constraints were dealt with by the penalty function method. 8-node hexahedral elements were employed.

3.2 One cross section analysis following FE bending [BndCr]

The second model (BndCr, bending and cross section) was also composed of two steps as shown in Figure 5. Step 1 is the same to that of Model [F-Expl], and the distribution of axial strains $\varepsilon_u(z)$ on the upper side and $\varepsilon_d(z)$ on the down side were extracted and transferred to Step 2. Step 2 calculated curvature distribution $c(z)$, axial strain distribution $\varepsilon_{ax(x,y,z)}$, axial stress distribution $\sigma_{ax(x,y,z)}$, and Moment distribution $M(z)$ in order. The detailed procedure is shown in Figure 6, and the meanings of the symbols are shown in Table 4. This model assumed that the bar shape should be kept just as the bent shape at Step 1, and calculated the strain and stress history. Kinematic hardening and Bauschinger effect were not taken into account. The curvatures c_{ex} and c_{ey} after spinner straightening were determined so that the moment, which is the integration value of axial stress σ_{ax}, should be zero.

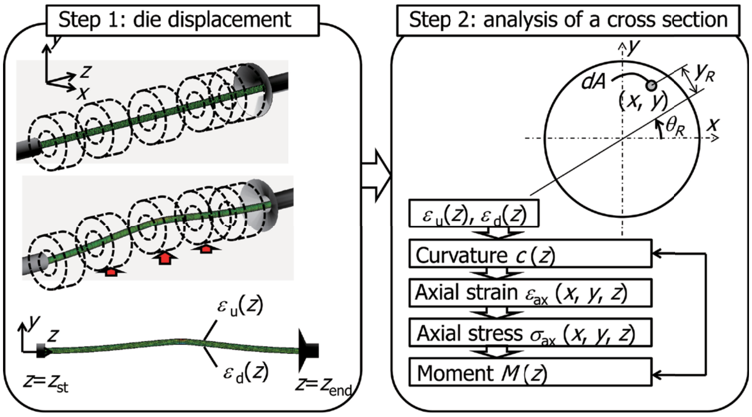

Figure 5: Analysis steps in model [BndCr]

Table 4: Notation

$\phi(k)$	initial curvature direction	z	axial position	z_{st}	start position
z_{end}	end position	c	curvature	ε_{el}	elongation strain
c_x	curvature in x	c_y	curvature in y	ε_{ax}	axial strain
σ_{ax}	axial stress	M_x	moment around x axis	M_y	moment around y axis
c_{ex}	curvature around x axis	c_{ey}	curvature around y axis	c_S	short-span curvature
c_L	long-span curvature	d_b	bar diameter		

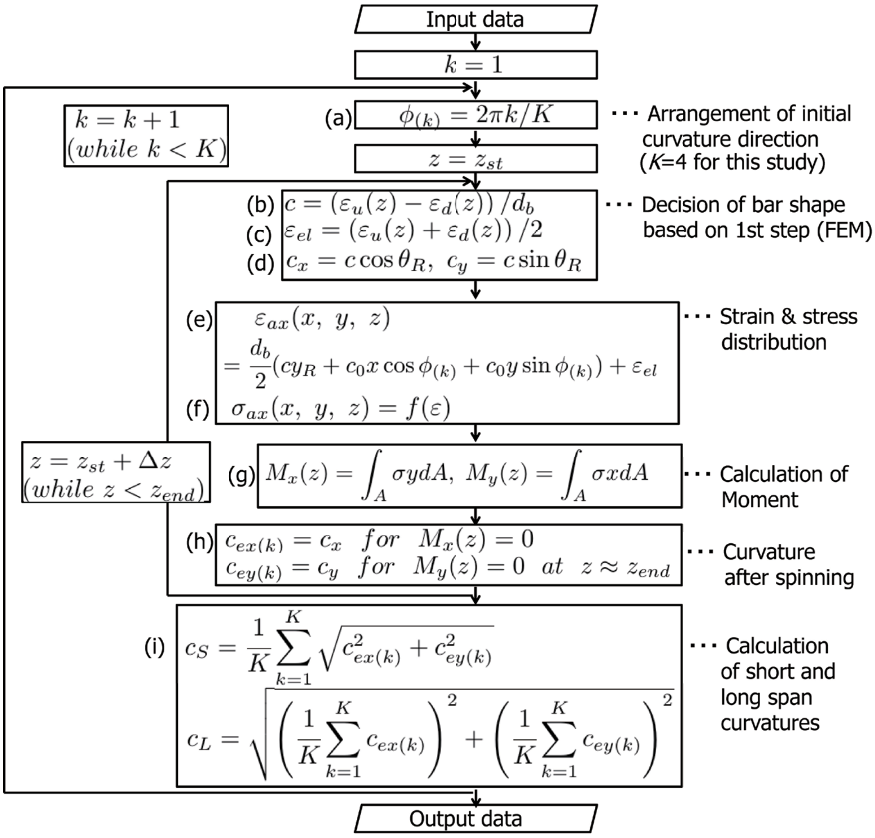

Figure 6: Flow chart for 2nd step in model [BndCr]

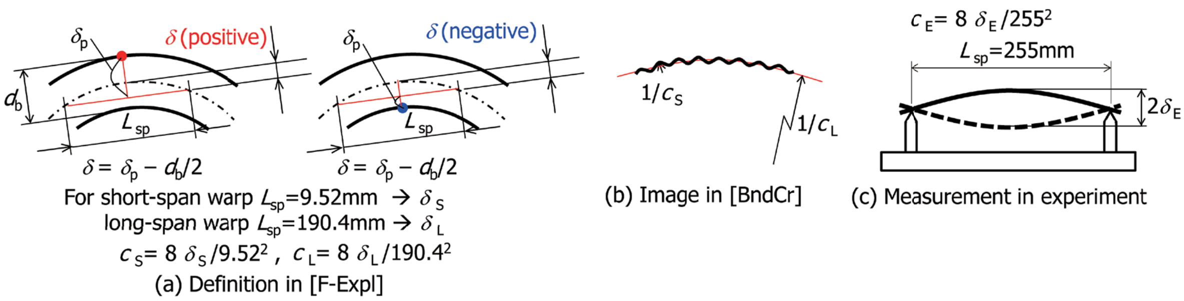

Figure 7: Curvature

3.3 Evaluation of straightness

Curvature was used for the evaluation of straightness, and was defined as shown in Figure 7. Model [F-Expl] can show curvature distribution. The curvature was calculated for each node as shown in Figure 7(a). When the value was positive, the node was placed on the extrados of the bar arc. When it was negative, the node was on the intrados. The chord lengths L_{sp} were set to be 9.52 mm (feed pitch f) and 190.4 mm ($10f$) for evaluation of short-span curvature c_S and long-span curvature c_L. In Model [BndCr], the short-span curvature c_S and long-span curvature c_L were calculated by equations in Figure 6. The image of c_S and c_L are shown in Figure 7(b). The long span curvature c_E was measured in the experiment as shown in Figure 7(c).

4 ANALYTICAL AND EXPERIMENTAL RESULTS

4.1 Results in full explicit scheme model (F-Expl)

Model [F-Expl] shows the dynamic shape change during spinner straightening. Figure 8 shows the curvature distribution during spinner straightening under the condition of Table 1[B]. "Initially intrados line"in (a) means the intrados line of the curved bar with curvature of c_0 in Figure 3. The bar started to be twisted at Die #3. The short-span curvatures periodically generated at Die #3.

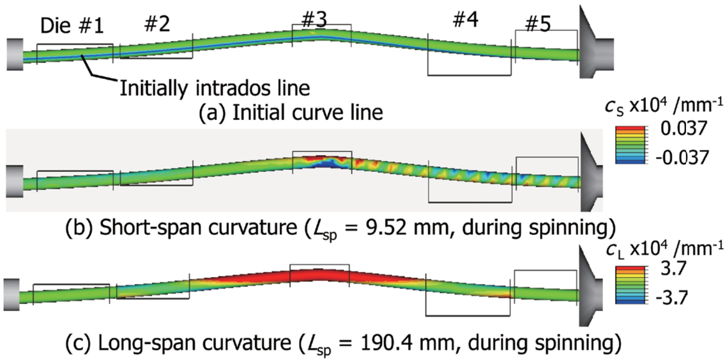

Figure 8: Spiral and warp during spinner straightening under the condition of Table 1[B]

Figure 9 shows the curvature distribution after spinner straightening under the condition of Table 1[B]. It is noteworthy that the extrados (red part) and the intrados (blue part) are found to be inconsistent before and after spinner straightening by comparing (a) and (c). In other words, the initial curvature was eliminated by spinner straightening. On the other hand, short-span curvatures periodically exist as shown in (b). If these curvatures c_S cancel each other, the long-span curvature c_L should be leveled to zero. However, the c_S did not cancel each other, and then c_L appeared.

Figure 10 shows the effect of Die #3 position h_3 on the curvature after spinner straightening. The curvatures c_L and c_E increased with increase of h_3. The model [F-Expl] and experimental results qualitatively show the same results. The spinner conditions in Table 1 might be strong enough for the elimination of the initial curvature, and these conditions would be called as "over straightening". As the result, the large h_3 caused large short-span curvature c_S, resulting in large long-span curvature c_L. The experimental results also showed that the effect of residual stress before spinner straightening on straightening effect was small as the difference between [a] (2-pass drawing: very small residual stresses) and [b] (1-pass drawing) was small. Figure 11 shows the effect of Die #3 position h_3 on twist in spinner straightening. The bars were twisted at Die #3. The spiral angle ϕ

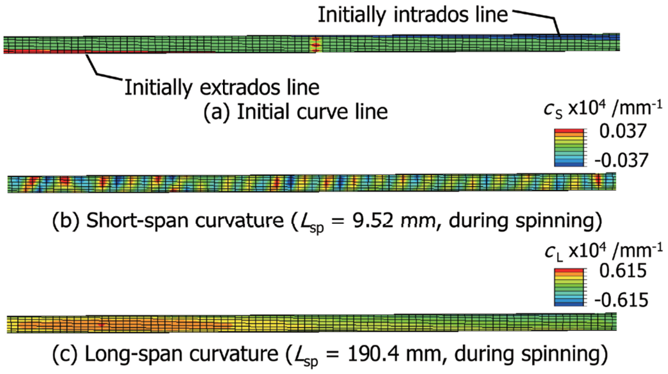

Figure 9: Spiral and warp after spinner straightening under the condition of Table 1[B]

increased with increase of h_3.

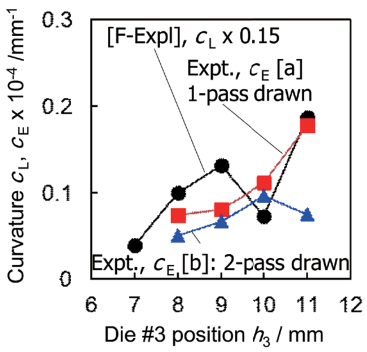

Figure 10: Effecti of die position on curvatures in [F-Expl] and experiment

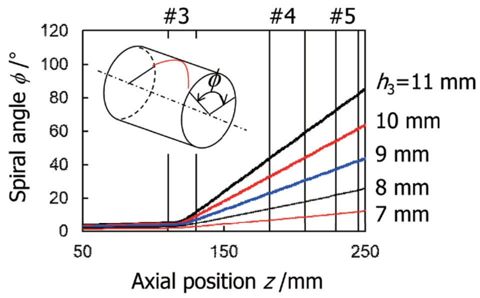

Figure 11: Effect of die position on twist in bar bar obtained by [F-Expl]

4.2 Results in one cross section analysis following FE bending [BndCr]

Model [BndCr] shows the results, which is obtained based on the statically bent bar. Figure 12 shows the effect of Die #3 position h_3 on the curvature after spinner straightening. The analytical long-span curvature c_L decreased with increase of h_3 against the experimental one c_E. On the other hand, the analytical short-span curvature c_S qualitatively show the same tendency to c_E. 0.06 times c_S might be used for the prediction of the experimental long-span curvature c_E. In the static model [BndCr], the local curvatures would cancel each other, and then the long-span curvature c_L decreased with increase of h_3. However, in the experiment, the local curvature do not completely cancel each other, excessive h_3 lead to large curvature c_E.

The mechanism in spinner straightening would be depicted as in Figure 13. When Die #3 position h_3 is small, the initial long-span curvature should exist as (a). When h_3 is appropriate, short-span curvatures or waves periodically appears eliminating the initial long-span curvature as (b). When h_3 is excessively large, the short-span curvatures are large as (c). If the short-span curvatures cancel each other, the long-span curvature would be kept at the small value as (c1). However, they do not cancel each other in practice, and then the long-span curvature becomes large as (c2).

The residual axial stresses are shown in Figure 14. Under the conditions in this study, the residual stress increased with increase of Die #3 position h_3. In other words, the residual stress increased with increase of long-span curvature c_E in the experiment.

These results show a fundamental guideline for spinner straightening, i.e. it is important to give minimum bare bending intensity to the bent part. Excessive intensity leads to secondary increase of long-span curvature as well as residual stresses.

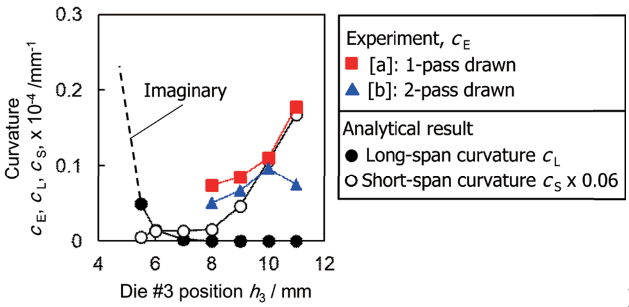

Figure 12: Curvatures in [BndCr] and experiment

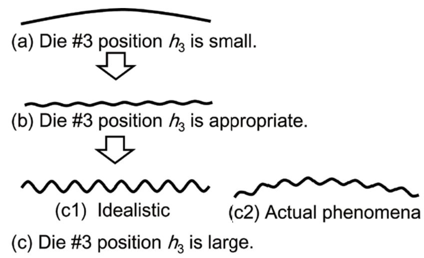

Figure 13: Mechanism for curvature generation

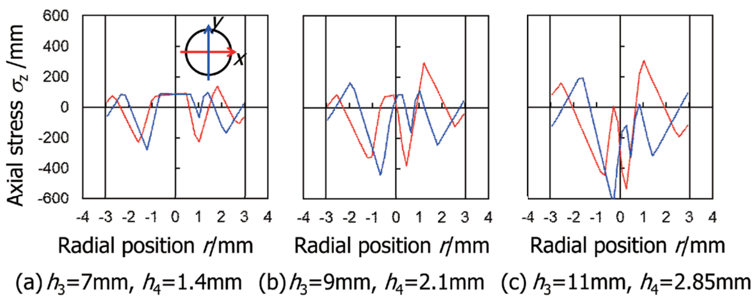

Figure 14: Residual stress after spinner straightening

5 CONCLUSIONS

- This paper presents two analytical models. One is Model [F-Expl] and the other is Model [ExplCr].
- [F-Expl] almost fully reproduced the movement of spinner straightening using the explicit scheme.
- [F-Expl] shows the distribution of both short and long span curvatures in a visual way.

- [F-Expl] showed that long-span curvature increased with increase of Die #3 position, or the increase of the intensity of straightening under the conditions of this study. This analytical tendency is qualitatively the same to that in experiment.
- [ExplCr] analyzed one-cross section based on the simple and static bending of the bar.
- [ExplCr] showed that 0.06 times calculated short-span curvature is the same level of long-span curvature in the experiment. Therefore, the 0.06 times the value might be used for prediction of the experimental curvature for the optimization of straightening condition.
- [ExplCr] showed residual stress might increase with increase of curvature in the experiment.
- Experimental curvature increased with increase of the bending intensity in this study. It would be attributed to the increase of short-span curvatures, which do not cancel each other.
- A fundamental guideline for spinner straightening was obtained, i.e. it is important to give minimum bare bending intensity to the bent part. Excessive intensity leads to secondary increase of long-span curvature as well as residual stresses.

REFERENCES

[1] Yanagihashi, T., Hama, T., Onoda, Y., Asakawa, M. Effect of plastic ratio and repeat bending on straightness in two-roll straightening - higher straightening and lower residual stress technology of bar products 3 -, *J. Jpn. Soc. Technol. Plast.*, (2005), **46**-537:972-976,in Japanese.

[2] Mutrux, A., Berisha, B., Weber, M., Hora, P. Fe simulation of cross roll straightening:, *COMPLAS X*, (2009) Barcelona, 23 in Index.

[3] Furugen, M., Hayashi, C. *Proc. 3rd. Int. Conf. Steel Rolling*, (1985) Tokyo, 497.

[4] Kuboki, T., Huang, H., Murata, M., Yamaguchi, Y., Kuroda, K. Fem analysis of tube straightener adopting implicit scheme, *Steel Research Int.*, (2010) **81**-9:584-587.

[5] Wu, B., Chan, L., Lee, T., Ao, L. A study on the precision modeling of the bars produced in two cross-roll straightening, *J. Mater. Process. Technol.*, (2000) **99**:22-206.

[6] Tsurumi, K., Asakawa, M., Kato, N., Urabe, M., Yoshida, M., Sakumoto, K., Kanno, T. *J. Jpn. Soc. Technol. Plast.*, (2014), **55**-640:435-439,in Japanese.

[7] Kuboki, T., Akiyama, M., Neishi, Y., Kuroda, K. Effect of final drawing with light reduction on the levelling of residual stress distribution in cold bar drawing, *Proc. Instn Mech. Engrs, Part C, J. of Mech. Eng. Sci.*, (2000) **214**-12:1389-1400.